Struct Bond (2017) 173: 97–120
DOI: 10.1007/430_2016_13

Hydrothermal Synthesis of Lanthanide and Lanthanide-Transition-Metal Cluster Organic Frameworks via Synergistic Coordination Strategy

Jian-Wen Cheng and Guo-Yu Yang

Abstract The study of polynuclear lanthanide (Ln) complexes has been a field of rapid growth in coordination chemistry. Lanthanide clusters synthesized via a ligand-controlled hydrolytic approach using different flexible α-amino acids have been well summarized. In this chapter, we describe efforts to synthesize lanthanide and lanthanide-transition-metal (Ln-TM) cluster organic frameworks using rigid ligands of isonicotinic acid (HIN), 4-pyridin-4-ylbenzoic acid (HL), nicotinic acid (HNA), and 4-(3-pyridyl)benzoic acid (HL′) under hydrothermal condition. In addition, the synergistic coordination between these rigid ligands with other organic/inorganic ligands has also been discussed.

Keywords Heterometallic compounds • Hydrothermal synthesis • Lanthanide cluster organic framework • Rigid ligands • Synergistic coordination

Contents

J.-W. Cheng and G.-Y. Yang (✉)
MOE Key Laboratory of Cluster Science, School of Chemistry, Beijing Institute of Technology, Beijing 100081, China

Key Laboratory of the Ministry of Education for Advanced Catalysis Materials, Institute of Physical Chemistry, Zhejiang Normal University, Jinhua, Zhejiang 321004, China
e-mail: ygy@bit.edu.cn

Abbreviations

2,5-pdc	2,5-Pyridinedicarboxylic acid
H_2bdc	1,2-Benzenedicarboxylic acid
HIN	Isonicotinic acid
HL	4-Pyridin-4-ylbenzoic acid
HL′	4-(3-Pyridyl)benzoic acid
HNA	Nicotinic acid
HOAc	Acetic acid
Ln	Lanthanide
ox	Oxalate
TM	Transition metal

1 Introduction

Lanthanide (Ln) and lanthanide-transition-metal (Ln-TM) clusters and coordination polymers are of great interest because of their fascinating structures and a variety of applications ranging from luminescent and magnetic materials to their use in homogeneous catalysis [1–7]. At present, hydroxo lanthanide clusters can be synthesized via a ligand-controlled hydrolytic approach with the judiciously chosen supporting ligands to limit the degree of lanthanide hydrolysis and the aggregation of the hydroxo intermediates [8, 9]. To date, a large number of lanthanide clusters from Ln_3 to Ln_{104} have been reported [10–25], in which most of the reported high-nuclearity hydroxo lanthanide clusters are discrete. Obviously, novel lanthanide clusters with interesting structures and exciting properties strongly rely on the innovations in synthetic methodology, developing new synthetic methods continue to be of great importance in this field. Hydrothermal synthesis represents a kind of milder and softer synthetic techniques by employing water as reaction media at relatively low temperature. Hydrothermal synthesis has been widely used in the synthesis of coordination polymers or metal–organic frameworks [26, 27], and extended to grow crystalline lanthanide cluster organic frameworks very recently [28]. Under hydrothermal process, lanthanide oxides can be used as the source of lanthanides in the presence of acid at low pH value, rather than using lanthanide salts in aqueous solution at high pH value.

The coordination chemistry of the copper(I) halides has been of great interest due to their large structural variation and rich electronic/optical properties. Copper (I) halides are inclined to form a variety of inorganic CuX clusters generally based on corner or edge sharing of trigonal planar $\{CuX_3\}$ or tetrahedral $\{CuX_4\}$ subunits, various copper halide cluster motifs from rhomboid Cu_2X_2 dimers, cubane or stepped cubane Cu_4X_4 tetramers to $Cu_{36}X_{56}$ have been well documented [29]. Therefore, it should be rational to introduce CuX clusters into the Ln cluster organic framework to construct fascinating 3D hetero-Ln-TM structures. Linear and rigid ligands with oxygen and nitrogen donors, such as isonicotinic acid (HIN)

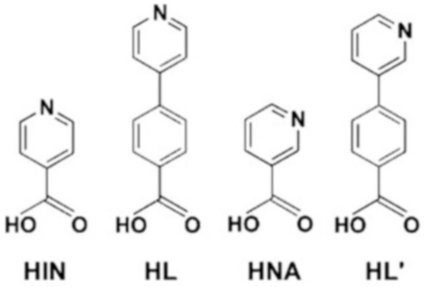

Scheme 1 Pyridyl benzoate ligands discussed in this chapter

and 4-pyridin-4-ylbenzoic acid (HL) were selected to make lanthanide and Ln-TM cluster organic frameworks based on the following considerations: (1) They are rigid ligands with oxygen and nitrogen donors on opposite sides, enabling these ligands to act as a linear bridge for the formation of the extended structures. (2) The carboxy group may induce the oxophilic lanthanide ions to undergo hydroxo lanthanide cluster aggregation, while the nitrogen atoms can coordinate to TM ions, and thus extended solids containing hydroxo lanthanide cluster cores and TM ions might be obtained. The hetero-Ln-TM structures consist of both Ln^{3+} and d ^{10} TM ions (Cu/Ag/Zn), which may expand their applications in photovoltaic and optoelectronic devices, based on their luminescent properties [4]. In addition, the synergistic coordination between HIN/HL and other organic/inorganic ligands also gives rise to a new series of lanthanide cluster organic frameworks. Lanthanide cluster organic frameworks constructed by the analogue nicotinic acid (HNA) and 4-(3-pyridyl)benzoic acid (HL′) have also been discussed (Scheme 1).

2 Lanthanide and Lanthanide-Transition-Metal Cluster Organic Frameworks

2.1 Cluster Organic Frameworks Constructed by Isonicotinic Acid

Hydrothermal reaction of Ln_2O_3, HIN, and $CuCl_2 \cdot 2H_2O$ in water in the presence of $HClO_4$ (pH 2) leads to three lanthanide cluster organic frameworks: $[Ln_{14}(\mu_6\text{-}O)(\mu_3\text{-}OH)_{20}(IN)_{22}Cu_6Cl_4\ (H_2O)_8] \cdot 6H_2O$ (Ln = Y, Gd, Dy) [30]. These structures contain the high-nuclearity hydroxo lanthanide cluster $[Ln_{14}(\mu_6\text{-}O)(\mu_3\text{-}OH)_{20}(H_2O)_8]^{20+}$, which acts as a building block that combines with copper ions through linear IN^- ligands to form a 3D framework. The Gd_{14} core consists of one octahedral $[Gd_6(\mu_6\text{-}O)(\mu_3\text{-}OH)_8]^{8+}$ unit that shares two opposing Gd1 apexes with two novel $[Gd_5(\mu_3\text{-}OH)_6]^{4+}$ trigonal bipyramids. The linkages between the Gd_{14} cores and two different types of copper centers through IN^- ligands give rise to an unusual 3D cluster organic framework (Fig. 1).

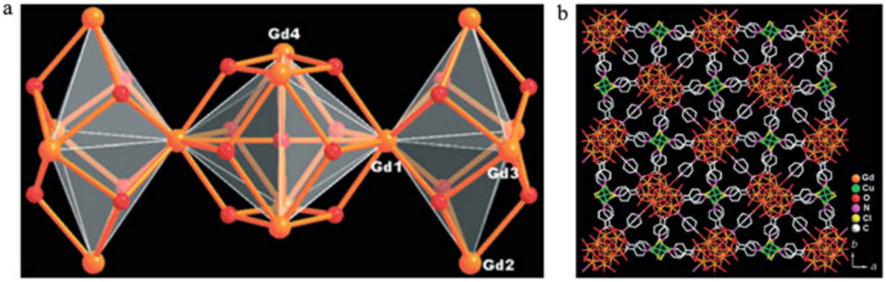

Fig. 1 (**a**) Polyhedral representation of the structure of $[Gd_{14}(\mu_6\text{-}O)(\mu_3\text{-}OH)_{20}]^{20+}$ core; (**b**) the overall 3D structure showing the unusual framework. Reproduced from [30] by permission of John Wiley & Sons Ltd

The I^- ion has a larger ionic radius than Cl^- and Br^-, and may favor higher coordination numbers and versatile coordination modes, resulting in a larger copper-iodide cluster. Hydrothermal reactions of Ln_2O_3, CuI, HIN, and 2-pyrazinecarboxylic acid in water in the presence of $HClO_4$ (pH 2) give the sandwich frameworks: $[Ln_6(\mu_3\text{-}O)_2](IN)_{18}[Cu_8(\mu_4\text{-}I)_2(\mu_2\text{-}I)_3] \cdot H_3O$ (FJ-4, Ln = Y, Nd, Dy, Gd, Sm, Eu, Tb) [31]. Two unusual trinuclear $[Ln_3(\mu_3\text{-}O)]$ and tetranuclear $[Cu_4(\mu_4\text{-}I)]$ cores are successfully used as secondary building units to make two different nanosized wheels $[Ln_{18}(\mu_3\text{-}O)_6(CO_2)_{48}]^{6-}$, Ln_{18}, and $[Cu_{24}(\mu_4\text{-}I)_6(\mu_2\text{-}I)_{12}]^{6+}$, Cu_{24}, with 12-membered rings and a diameter of 26.7 and 26.4 Å, respectively. The wheels are further assembled into 2D Ln_{18} and Cu_{24} networks, the linkages between two distinct layered networks of Ln_{18} and Cu_{24} wheels by IN^- pillars along the *c* axis giving a series of unprecedented 3D sandwich frameworks (Fig. 2).

$Dy_{30}I(\mu_3\text{-}OH)_{24}(\mu_3\text{-}O)_6(NO_3)_9(IN)_{41}(OH)_3(H_2O)_{38}$ and $Dy_{104}I_4(\mu_3\text{-}OH)_{80}(\mu_3\text{-}O)_{24}(NO_3)_{36}(IN)_{125}(OH)_{19}(H_2O)_{167}$ have been obtained under hydrothermal conditions by incorporation of IN^- and $NO_3{}^-$ ligands [32]. $[Dy_{26}(\mu_3\text{-}OH)_{20}(\mu_3\text{-}O)_6(NO_3)_9I]^{36+}$ cluster core motif has been observed in their crystal structures, nine $NO_3{}^-$ ligands are incorporated into the cluster core backbone by Dy–O coordination bonds. The size of the Dy_{26} cluster is 20.47 × 17.20 $Å^2$. The synergistic coordination between the IN^- ligands and the trigonal planar geometry $NO_3{}^-$ ligands as surface modifiers inserted into the lanthanide cluster core backbone remarkably improves the dimension of cluster cores.

$Dy_{30}I(\mu_3\text{-}OH)_{24}(\mu_3\text{-}O)_6(NO_3)_9(IN)_{41}(OH)_3(H_2O)_{38}$ consists of two Dy_{26} and two Dy_4 clusters, these clusters are further linked by IN^- linkers to form the final structure, while $Dy_{104}I_4(\mu_3\text{-}OH)_{80}(\mu_3\text{-}O)_{24}(NO_3)_{36}(IN)_{125}(OH)_{19}(H_2O)_{167}$ is the first tetramer assembled by the Dy_{26} clusters and IN linkers (Fig. 3).

Compared with the reported discrete Ln_{26} cluster of $[Dy_{26}(\mu_3\text{-}OH)_{20}(\mu_3\text{-}O)_6(NO_3)_9I]^{36+}$ [32], Xu et al. replaced $NO_3{}^-$ by $CO_3{}^{2-}$ to reinforce the huge Ln_{26} cluster and introduced a third ligand CH_3COO^- to reduce the steric restriction.

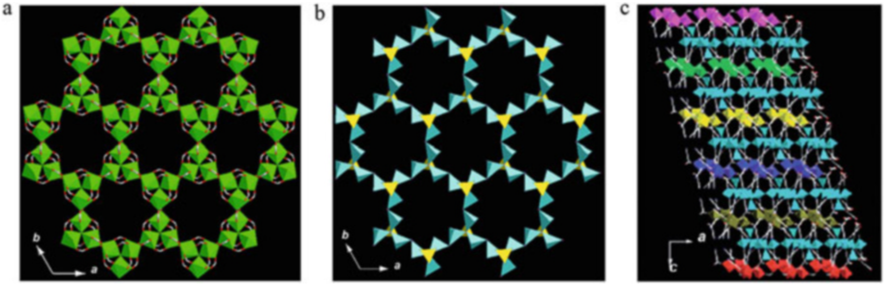

Fig. 2 (**a**) Polyhedral view of layered network of Dy_{18} wheels; (**b**) polyhedral view of layered network of Cu_{24} wheels; and (**c**) view of the layered networks of Dy_{18} and Cu_{24} wheels linked by IN^{-} ligands. Reproduced from [31] by permission of John Wiley & Sons Ltd

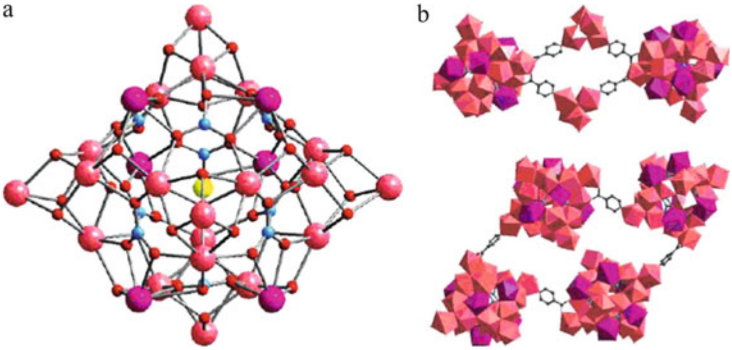

Fig. 3 (**a**) View of the structure of Dy_{26} core; (**b**) view of the structures of tetramer constructed by lanthanide clusters and IN^{-} linkers. Reprinted with the permission from [32]. Copyright 2007 American Chemical Society

Two 3D coordination polymers $Zn_{1.5}Dy_{26}(IN)_{25}(CH_3COO)_8(CO_3)_{11}(OH)_{26}(H_2O)_{29}$ and $Zn_{1.5}Gd_{26}(IN)_{26}(CH_3COO)_7(CO_3)_{11}(OH)_{26}(H_2O)_{28}$ have been hydrothermally synthesized [33]. Structural analysis indicates that the ligands IN^{-}, CH_3COO^{-}, and $CO_3{}^{2-}$ anion make the Ln_{26} cluster stable. The linkages between nanosized Ln_{26} cluster and Zn centers through IN ligands result in two novel 3D open framework topologies (Fig. 4).

A novel 2D coordination polymer $K_2[Ho_{48}(IN)_{46}(\mu_3\text{-}OH)_{84}(\mu_4\text{-}OH)_4(\mu_5\text{-}O)_2(OAc)_4(H_2O)_{14}(CO_3)Br_2]\cdot 2HIN\cdot 20H_2O$ [34] which contains nanosized Ho_{48} clusters was synthesized and structurally characterized by Xu et al. At the top or bottom of the core structure of Ho_{48}, each cubane-like $[Ho_4(\mu_3\text{-}OH)_4]^{8+}$ unit (Fig. 5a) can be described as a tetrahedron, while the middle Ho_5 (Fig. 5b) units can be depicted as square pyramids. Six Ho_5 units surround the equatorial ring of the

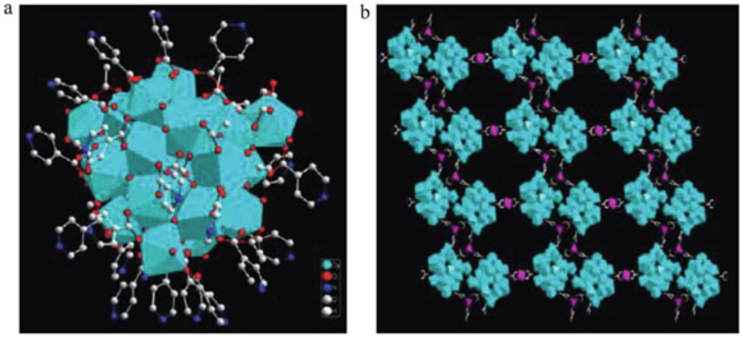

Fig. 4 (**a**) View of the Ln_{26} core; (**b**) the linkages of nanosized Ln_{26} clusters and zinc centers by IN^- ligands. Reprinted with the permission from [33]. Copyright 2010 American Chemical Society

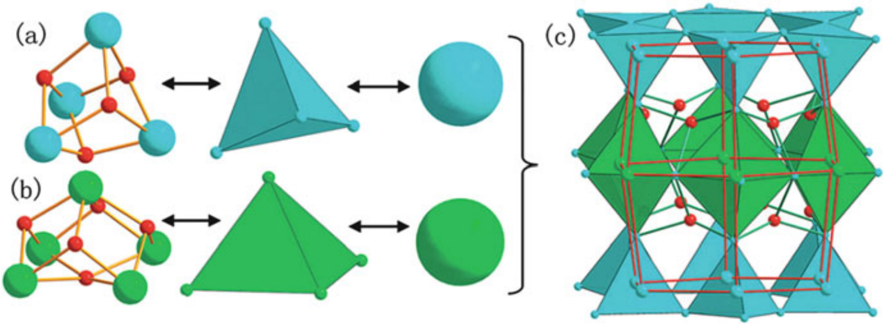

Fig. 5 (**a**) The $\{Ho_4\}$ cluster unit. (**b**) The $\{Ho_5\}$ cluster unit. (**c**) The drum-like core structure of $\{Ho_{48}\}$ cluster. Reproduced from [34] by permission of The Royal Society of Chemistry

Ho_{48} core via six corner sharing Ho atoms to form the barrel of the drum (Fig. 5c). Each Ho_{48} cluster is simultaneously bridged to four adjacent Ho_{48} cores by the IN^- ligands to form a large rhombic ring with a length of 26.57 Å (Fig. 6). Similar nanosized Ln_{48} cluster is also observed in $\{[Cl_2\&(NO_3)]@[Er_{48}(NA)_{44}(OH)_{90}(N_3)(H_2O)_{24}]\}_n \cdot 6n Cl \cdot 35n H_2O$ [35], in which Er_{48} clusters are linked by NA^- ligands and N_3^- anions to give a square layer, Cl^- and NO_3^- anions act as templates.

Xue et al. obtained two 3D heterometallic coordination polymers, $Ln_4(\mu_3\text{-}OH)_2Cu_6I_5(IN)_8(OAc)_3$ (Ln = Nd, Pr; HOAc = acetic acid) under hydrothermal conditions [36]. The Ln_6 and Ln_2 cores are connected alternately to form a nanosized Ln_{16} wheel with an eight-membered ring with the size of 12.59 and

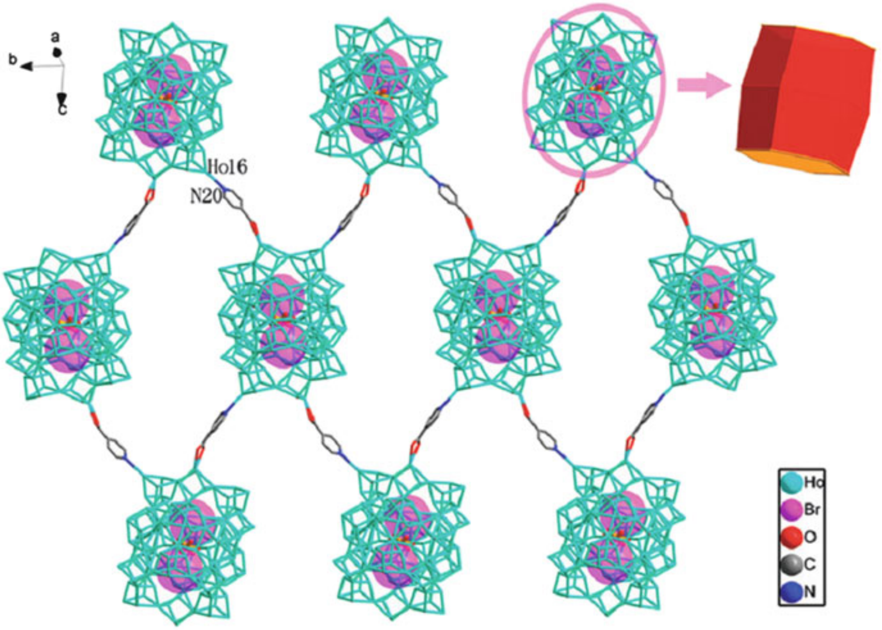

Fig. 6 The layered structure connected by IN ligands. Reproduced from [34] by permission of The Royal Society of Chemistry

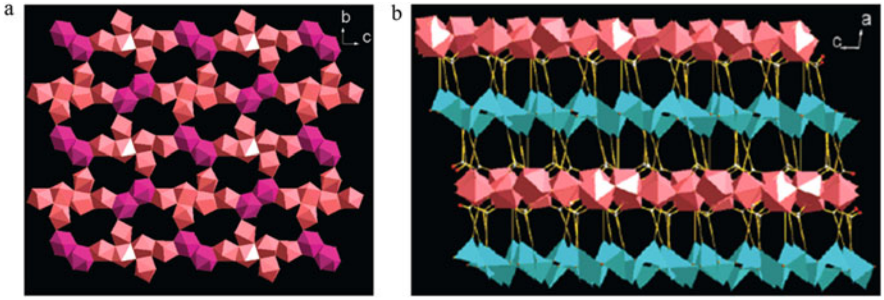

Fig. 7 (**a**) View of the 2D cluster network constructed by lanthanide wheel clusters with an eight-membered ring; (**b**) view of the 3D coordination framework based on the linkage of 2D neodymium cluster layers and 1D copper-iodine cluster chains by IN^- linkers. Reprinted with the permission from [36]. Copyright 2007 American Chemical Society

9.13 Å, OAc^- ligand shows two different coordination modes. The transition-metal cluster moiety is the 1D chain formed by Cu_6I_5 clusters. It is interesting that the linkage between the 2D lanthanide wheel cluster layers and the 1D copper halide cluster chains by IN^- ligands gives rise to a 3D coordination framework (Fig. 7).

If a second ligand 1,2-benzenedicarboxylic acid (H_2bdc) were to be introduced, the synergistic coordination between IN and bdc ligands leads to two new lanthanide cluster organic frameworks, $[Er_7(\mu_3\text{-}O)(\mu_3\text{-}OH)_6(bdc)_3](IN)_9[Cu_3X_4]$ (X = Cl/Br, FJ-2a/b) [37]. The Er_4 and the Er_2 cores are alternately linked from a nanosized $[Er_{36}(\mu_3\text{-}OH)_{30}(\mu_3\text{-}O)_6(bdc)_6]^{54+}$ (Er_{36}), this wheel-shaped building block of Er_{36} with an 18-membered ring is currently the largest lanthanide wheel (Fig. 8a). Remarkably, six bdc^{2-} ligands are trapped in the inner of the 18-membered ring (Fig. 8a). Each Er_{36} cluster is linked to surrounding clusters and forming a highly ordered layered cluster network with hexagonal, honeycomb arrays (Fig. 8b). The linkages between 2D hybrid cluster polymers and copper clusters by IN^- ligands give rise to an unprecedented 3D sandwich framework (Fig. 8c).

The synergistic coordination between IN^- and 2,5-pyridinedicarboxylic acid gives a new lanthanide cluster organic framework, $Er_4(OH)_4Cu_5I_4(IN)_6(NA)(2,5\text{-pdc})\cdot 0.3H_2O$ (HNA = nicotinic acid, 2,5-pdc = 2,5-pyridinedicarboxylic acid) [38]. This compound consists of two distinct building blocks of inorganic 1D $[Ln_4(OH)_4]_n^{8n+}$ cluster polymers and $[Cu_{10}I_8]^{2+}$ clusters. The inorganic 1D $[Ln_4(OH)_4]_n^{8n+}$ chains are further connected to each other by 2,5-pdc^{2-} into 2D

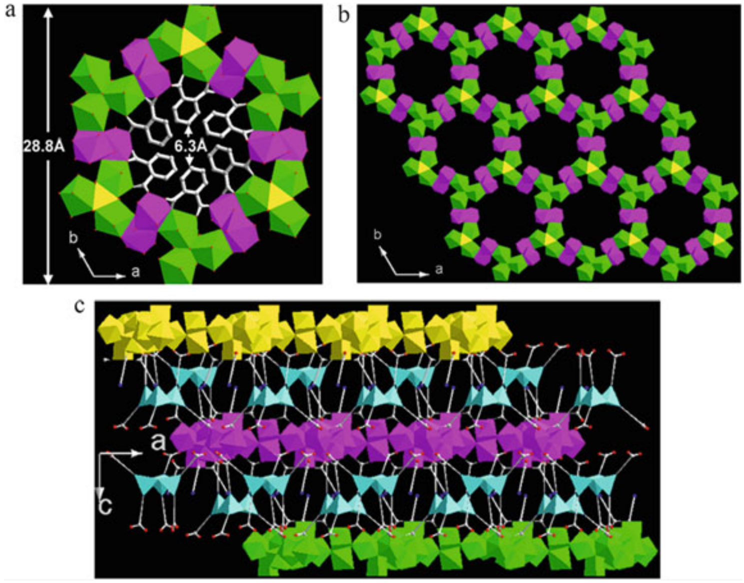

Fig. 8 (**a**) View of the Er_{36} wheel; (**b**) view of giant wheel clusters linked to form layered cluster network; and (**c**) view of sandwich framework based on linkages of 2D cluster layers and Cu cluster pillars by IN^- ligands. Reproduced from [37] by permission of John Wiley & Sons Ltd

layers in the *ab* plane. The linkage between layered Ln networks and $[Cu_{10}I_8]^{2+}$ clusters by IN^{-} and NA^{-} pillars along the *c* axis forms an unprecedented 3D framework (Fig. 9). It is interesting that decarboxylation occurred in the ortho position and 2,5-pdc^{2-} was partially transformed into NA^{-} under hydrothermal conditions.

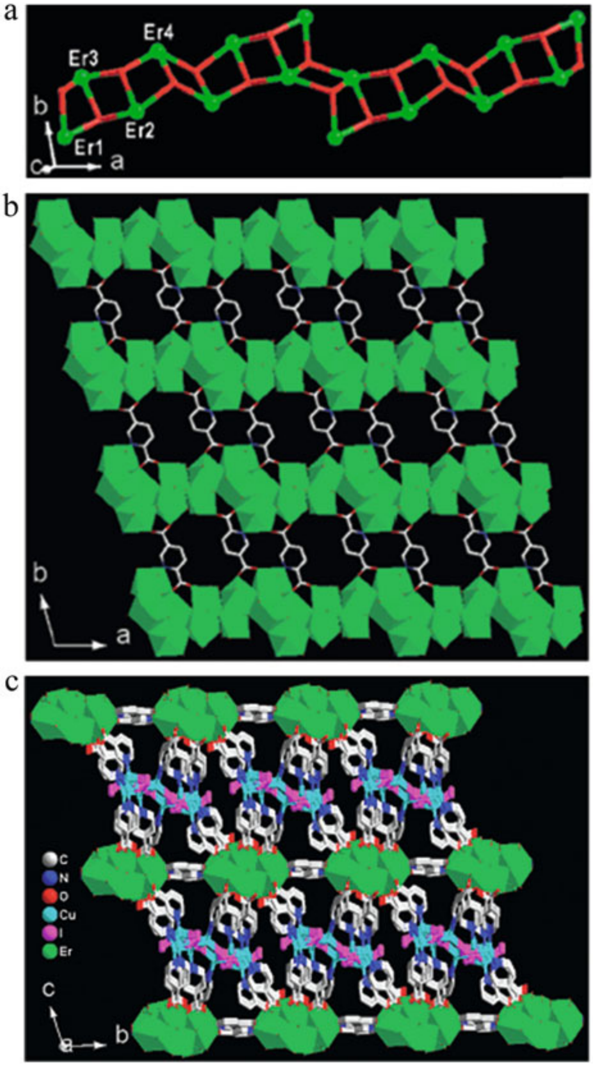

Fig. 9 (**a**) View of the inorganic $[Ln_4(OH)_4]_n^{8n+}$ chain; (**b**) 2D Ln–organic layer; and (**c**) the 3D framework. Reprinted with the permission from [38]. Copyright 2008 American Chemical Society

2.2 Cluster Organic Frameworks Constructed by 4-(4-Pyridyl)benzoic Acid

To make new Ln cluster organic frameworks for potential applications, an expanded ligand with a benzene spacer between the two coordinating moieties of HIN, 4-pyridin-4-ylbenzoic acid (HL), is employed, with the expectation that this lengthened ligand is capable of avoiding steric crowding around metal clusters. Heptanuclear trigonal-prismatic Ln clusters derived from HL, $[Ln_7(\mu_3\text{-}OH)_8L_9(H_2O)_6]\cdot 4ClO_4\cdot 3HL\cdot nH_2O$ (Ln = Y, La, Gd, Yb, $n = 6$; Ln = Dy, Er, $n = 4$), were made by the hydrothermal treatment of Ln_2O_3 and HL at 190°C for 7 days in the presence of $HClO_4$ (pH 2) [39]. The heptanuclear cluster core, $[Y_7(\mu_3\text{-}OH)_8]^{13+}$ (Y_7) core, can be described as two $Y_4(OH)_4$ cubanes sharing a Y atom, in contrast to previously reported trigonal antiprismatic Ln_7 cores [40]. In the structure, each Y_7 core connects six nearest neighbors with a distance of 16.955 Å by the ligands to produce a 2D Ln cluster organic layer possessing a thickness about 10.92 Å along the *b* axis (Fig. 10).

Two pillared-layer cluster organic frameworks, $[Ln_5(\mu_3\text{-}OH)_4(\mu\text{-}H_2O)Cu_8I_8L_{11}]\cdot H_2O$ (Ln = Dy, Eu), have been made by employing lanthanide oxide and copper(I) halide as the source of lanthanide and transitional metal under hydrothermal condition [41]. There are two distinct nanoscale crown-like clusters in the structure, one is hydroxo lanthanide $[Dy_{10}(\mu_3\text{-}OH)_8]^{22+}$ (Dy_{10}) cluster and the other is copper(I) halide $[Cu_{16}I_{16}]$ (Cu_{16}) cluster. The Dy_{10} cluster can be intuitively regarded as a slightly slipped sandwich configuration. Each half of the sandwich contains a roughly planar set of five Dy^{3+} ions in a trapezoid arrangement, which can be viewed as three edge-sharing triangles with each bearing a capped μ_3-OH group. The Dy_{10} core has an external diameter of 1.2 nm and an inner olive-shaped 4-ring with a diameter of 0.7 nm. The Dy_{10} cores are bridged by water molecules to

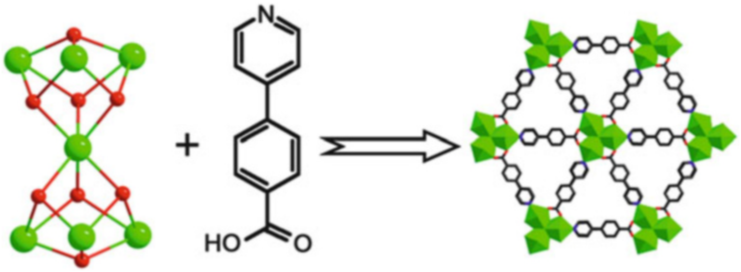

Fig. 10 View of the 2D Ln cluster organic layer constructed by Y_7 cluster and L^-. Reprinted with the permission from [39]. Copyright 2013 American Chemical Society

be a ribbon-like chain along the [0 1 0] direction. The adjacent inorganic chains with reverse orientation are extended via L^- ligands to generate Ln cluster organic layer on the *bc* plane. The Cu_{16} cores and the Ln cluster organic layers are pillared by the L^- ligands to generate a fascinating 3D pillared-layer cluster organic framework. From the topological point of view, these compounds represent an intriguing example of a binodal (8,14)-connected net considering the Dy_{10} and Cu_{16} connectors as the nodes, revealing that they are typical high dimensional frameworks with high connected net based on high-nuclearity nodes (Fig. 11).

The synergistic coordination between two different organic ligands, as well as inorganic and organic ligands, leads to two types of cluster organic frameworks: $[La_6(\mu_3\text{-}OH)_2(ox)_3L_{12}Cu_{11}(\mu_3\text{-}X)_6(\mu_2\text{-}X)_3]\cdot 8H_2O$ (X = Br/Cl, FJ-21 a/b; ox = oxalate); $[Ln_4(OAc)_3(H_2O)_4L_9][Cu(\mu_3\text{-}I)]@[Cu_{10}(\mu_3\text{-}I)\ (\mu_4\text{-}I)_6(\mu_5\text{-}I)_3]\cdot 7H_2O$ (Ln = Pr/Nd/Sm/Eu, FJ-22 a/b/c/d; OAc = acetate) [42]. FJ-21 a/b were made by hydrothermal treatment of lanthanum oxalate, CuX_2 (X = Br/Cl), and HL at 200°C for 5 days in the presence of $HClO_4$ (pH 2). The secondary building unit (SBU) of Ln wheel in FJ-21a is edge-sharing trinuclear unit $[La_3(\mu_3\text{-}OH)]^{8+}$ (La_3). Every La_3 core is linked by three ox ligands and nine L ligands. Six La_3 cores with reverse orientation are alternately linked by six ox ligands to form an $[La_{18}(\mu_3\text{-}OH)_6(ox)_6]^{36+}$ (La_{18}) wheel having a diagonal dimension of about 2.3 nm and a thickness of 0.4 nm, respectively. The SBU of CuI wheel in FJ-21a is Cu-centered edge-sharing truncated cubane $[Cu_4(\mu_3\text{-}Br)_6]^{2-}$. Six Cu_4 cores are connected by halide bridges into a nanosized neutral $[Cu_{24}(\mu_3\text{-}Br)_{18}(\mu_2\text{-}Br)_6]$ (Cu_{24}) wheel with 12-ring and a diameter of 2.0 nm. Two different kinds of the wheel cluster layers of La_{18} and Cu_{24} are pillared by L^- ligands to give rise to a 3D sandwich framework.

FJ-22 was made by hydrothermal reaction of Ln_2O_3, CuI, sodium acetate, and HL at low pH value under the same reaction conditions as FJ-21. The SBUs of Ln wheel in FJ-22d are edge-sharing tetranuclear $[Eu_4(OAc)_3]^{9+}$ (Eu_4) cores in

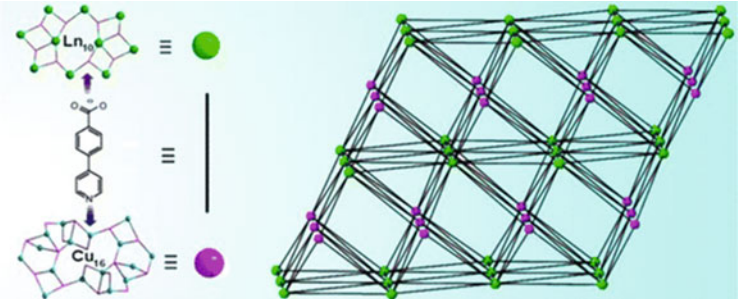

Fig. 11 View of the framework constructed by Dy_{10} and Cu_{16} clusters. Reprinted with the permission from [41]. Copyright 2014 American Chemical Society

compressed tetrahedral geometry. Six Eu_4 cores are alternately linked edge-to-edge by twelve L ligands to generate an $[Eu_{24}(OAc)_{18}(COO)_{12}]^{42+}$ (Eu_{24}) wheel with a diameter of 3.0 nm and a thickness of 0.4 nm. Six Cu_4 cores are linked alternately to form a nanosized $[Cu_{24}(\mu_4\text{-}I)_{12}(\mu_5\text{-}I)_6]^{6+}$ (Cu_{24}) wheel with 6-ring and a diameter of 2.8 nm. Therefore, the 3D sandwich framework of FJ-22d can be understood as the strictly alternating of Eu_{24} and Cu_{24} wheel cluster layers pillared by L ligands. Obviously, the synergistic coordination between organic ligands, L and oxalate/acetate, leads to the formation of La_{18} and Ln_{24} wheels, while the synergistic coordination between organic L and inorganic Br/I ligands results in Cu wheels for FJ-21 and FJ-22, respectively (Fig. 12).

Two sandwiched cluster organic frameworks, $Eu_6(OH)_2Cu_9I_6L_{12}(ox)_3 \cdot H_2O \cdot ClO_4$ (FJ-23, ox = oxalate) and $Eu_6Cu_7I_7L_{12}(OAc)_6(H_2O)_2 \cdot 2H_2O$ (FJ-24, OAc = acetate),

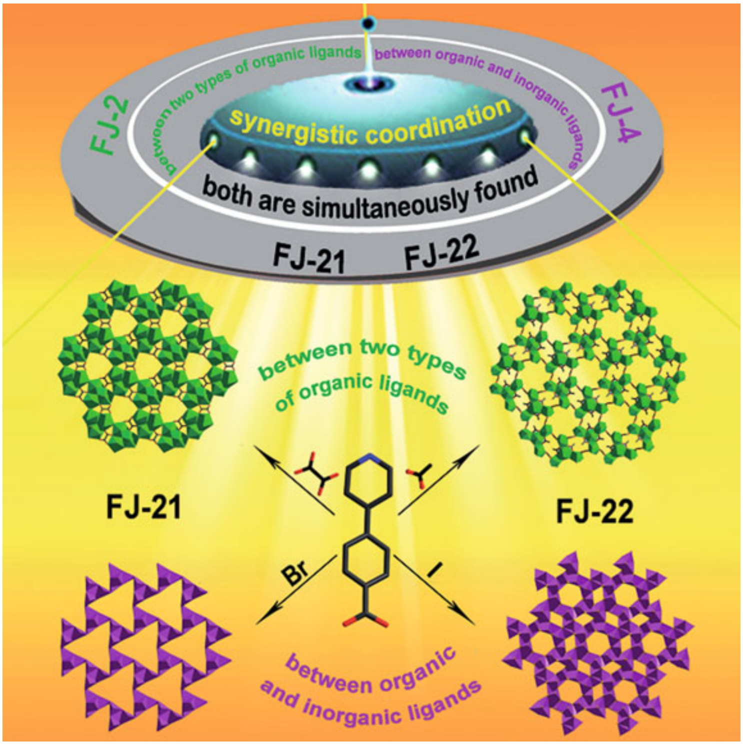

Fig. 12 The frameworks of FJ-21 and FJ-22 consist of two different kinds of nanosized Ln and Cu wheel cluster units. Reproduced from [42] by permission of John Wiley & Sons Ltd

have been successfully made [43]. In FJ-23, the $[Eu_{18}(\mu_3\text{-}OH)_6(ox)_6]^{36+}$ wheel contains six edge-to-edge equilateral triangles $[Eu_3(\mu_3\text{-}OH)]8+$ SBUs. While in FJ-24, the $[Eu_{18}(OAc)_{18}]^{36+}$ wheel is made up of six vertex-sharing compressed tetrahedral $[Eu_4(OAc)_3]^{9+}$ SBUs. In FJ-23 and FJ-24, the graphene-like wheel cluster layers are linked through shape-matching trigonal prism metalloligands into 5-connected BN nets (Figs. 13 and 14). The second harmonic generation (SHG) measurements show

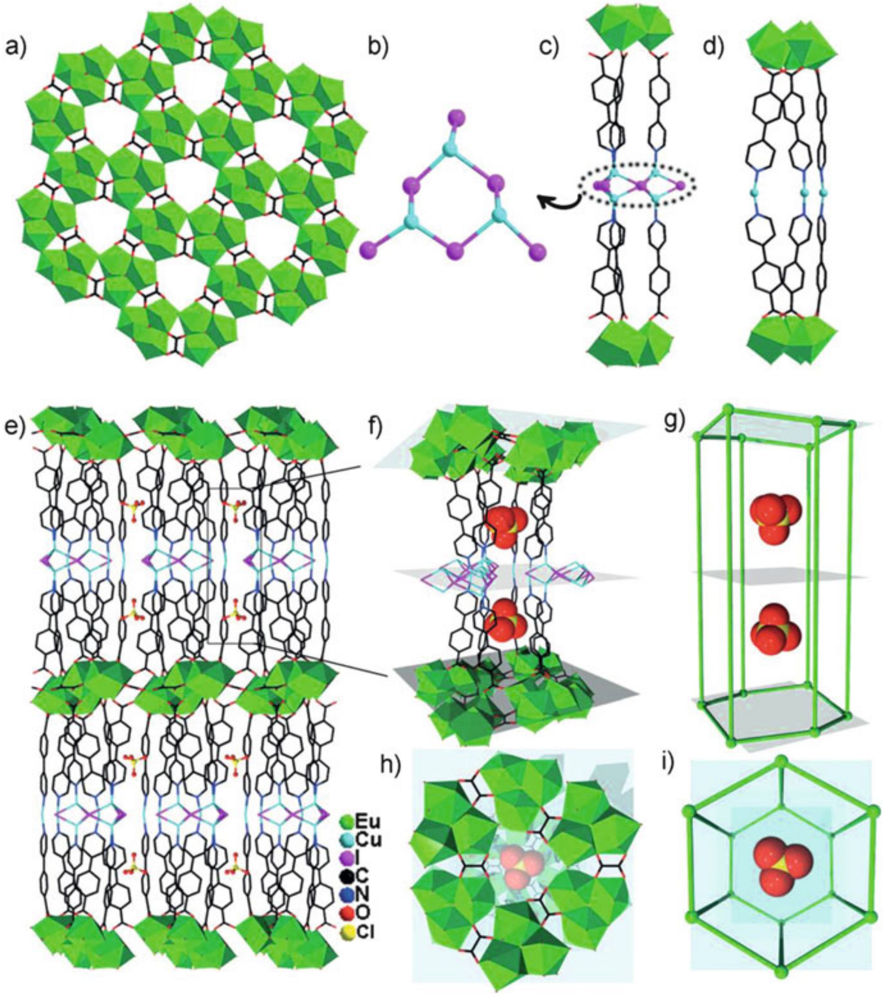

Fig. 13 (**a**) Polyhedral view of the graphene-like Eu_{18} wheel cluster layer in FJ-23; (**b**) ball/stick view of the Cu_3 SBU; (**c**, **d**) the coordinate environment of the Cu_3L_6 and $3(CuL_2)$ metalloligands in FJ-23; (**e**) the overall pillared-layer framework of FJ-23. (**f**–**i**) Zoomed images at the left show the side and top view of the ClO_4^- ions located in the narrow hexagonal channels. Reproduced from [43] by permission of John Wiley & Sons Ltd

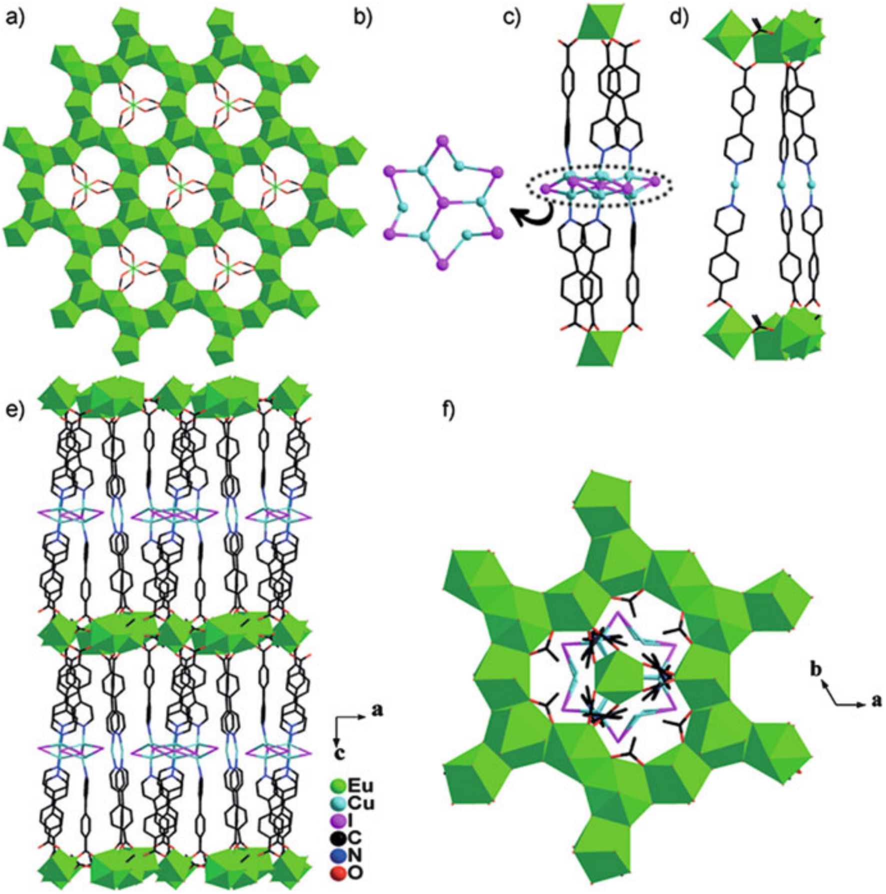

Fig. 14 (**a**) Polyhedral view of the Eu@Eu18 wheel cluster layer in FJ-24; (**b**) ball/stick view of the star-shape I@Cu_6 SBU; (**c**, **d**) the coordinate environment of the I@Cu_6L_6 and 3(CuL_2) metalloligands in FJ-24; (**e**) the overall pillared-layer framework of FJ-24; and (**f**) top view of the FJ-24. Reproduced from [43] by permission of John Wiley & Sons Ltd

that the SHG coefficients of FJ-23 and FJ-24 are about 0.15 and 0.2 times as large as that of KH_2PO_4 (KDP).

Two supertetrahedral cluster organic frameworks (SCOFs), $2(Ln_4Cu_{10}I_8L_{18})\cdot 8H_3O\cdot 9H_2O$ (Ln = Sm, Gd) were made by hydrothermal reaction of Ln_2O_3, CuI, and HL ligands at 180°C for 3 days [44]. A prominent structural feature of these two compounds is the presence of tetrahedral $[Sm_4(COO)_6]$ (Sm_4) and supertetrahedral

T$_3$-[Cu$_{10}$I$_8$] (Cu$_{10}$) clusters. Each Sm$_4$ tetrahedron is linked to six adjacent Cu$_{10}$ supertetrahedra via 18 carboxyl groups, and each Cu$_{10}$ supertetrahedron is bridged to six nearest Sm$_4$ tetrahedra by 18 pyridine nitrogen atoms, the overall framework exhibits a twofold interpenetrated pcu net (Fig. 15). The proton conductivity at 30°C is 7.1×10^{-6} S/cm at 30% RH. When the temperature increases to 80°C, the conductivity dramatically rises to 1.4×10^{-3} S/cm (Fig. 16).

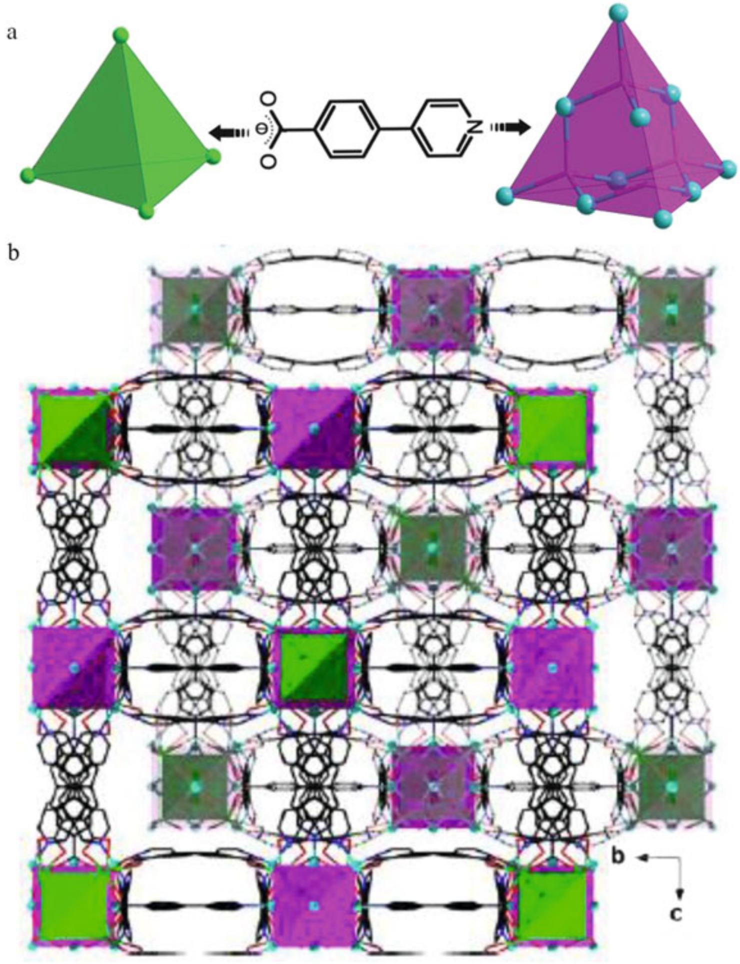

Fig. 15 (**a**) View of the inducement of Ln(III) tetrahedral and Cu(I) supertetrahedral clusters; (**b**) 3D framework along the *a*-axis. Reproduced from [44] by permission of John Wiley & Sons Ltd

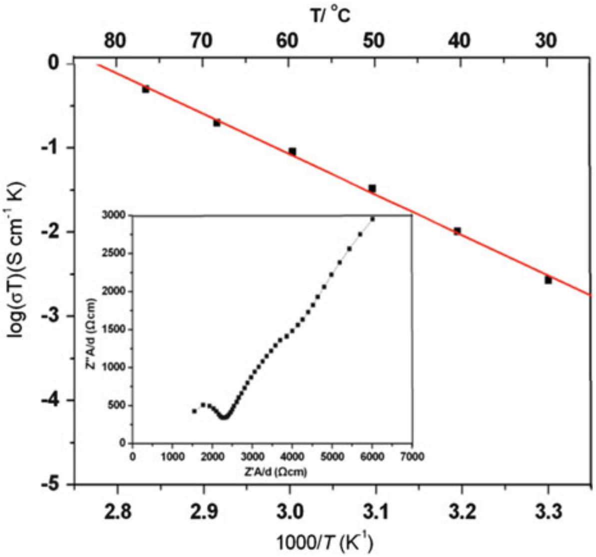

Fig. 16 Arrhenius plots of the proton conductivity under 95% RH. Reproduced from [44] by permission of John Wiley & Sons Ltd

2.3 Cluster Organic Frameworks Constructed by Nicotinic Acid

Koner et al. obtained a new Gd_{26} cluster based 3D framework, $\{[Gd_{26}(\mu_6\text{-}CO_3)_9(NA)_{32}(\mu_3\text{-}OH)_{26}](NO_3)_2 \cdot 3(H_2O)\}_n$ via hydrothermal synthesis [45]. Five distorted cubane cores are attached to each other through six Gd^{3+} ions to give the Gd_{26} clusters. The dimension of Gd_{26} cluster shell including the organic ligands is around 2.32(4) nm. The Gd_{26} clusters are then connected to each other by NA^- ligands forming a 3D framework. The compound catalyzes the heterogeneous epoxidation of olefinic substrates including α,β-unsaturated ketones (Fig. 17). Similar nanosized Ln_{26} clusters have been observed in lanthanide-transition-metal–organic frameworks, $[Dy_{26}Cu_3(NA)_{24}(CH_3COO)_8(CO_3)_{11}(OH)_{26}(H_2O)_{14}]Cl \cdot 3H_2O$ and $[Tb_{26}NaAg_3(NA)_{27}(CH_3COO)_6(CO_3)_{11}(OH)_{26}Cl(H_2O)_{15}] \cdot 7.5H_2O$ [46]. In these compounds, Ln_{26} clusters and Cu^+/$[Ag_3Cl]^{2+}$ centers are connected by NA^- bridges to give rise to 3D perovskite-like and 2D structures, respectively (Fig. 18).

Hong et al. reported two 2D coordination polymers based on huge 36-metal pure lanthanide clusters, $\{[Ln_{36}(NA)_{36}(OH)_{49}(O)_6(NO_3)_6(N_3)_3(H_2O)_{20}]Cl_2 \cdot 28H_2O\}_n$

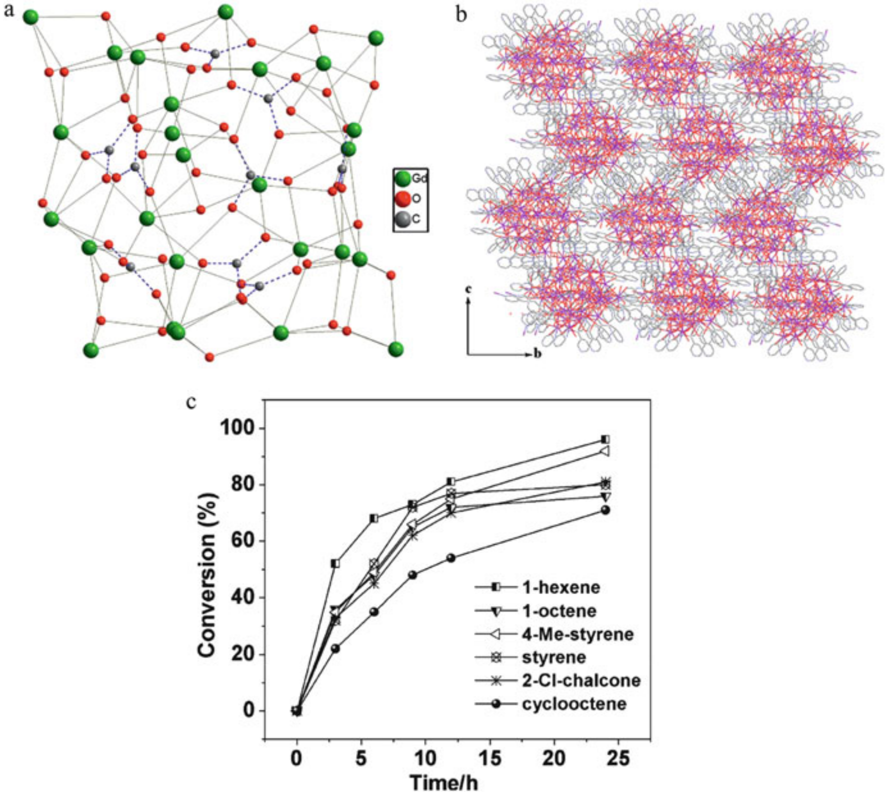

Fig. 17 (**a**) The structure of Gd_{26} cluster; (**b**) 3D framework along the *a*-axis; and (**c**) reaction profile for the epoxidation of olefins with *t*BuOOH catalyzed in acetonitrile media. Reproduced from [45] by permission of John Wiley & Sons Ltd

(Ln = Gd, Dy) [47]. Six tetrahedral Ln_4 clusters adopt an up and down arrangement and form a cyclohexane chair-like Ln_{24} cluster. The Ln_{36} cluster can be viewed as the aggregation of two types of cluster units of one wheel-like Ln_{24} unit and two identical tripod-like Ln_6 units (Fig. 19). The nanosized Ln_{36} clusters are then connected to each other by NA^- ligands to form a square layer. These compounds show a large MCE of 39.66 J kg^{-1} K^{-1} and slow relaxation of the magnetization, respectively.

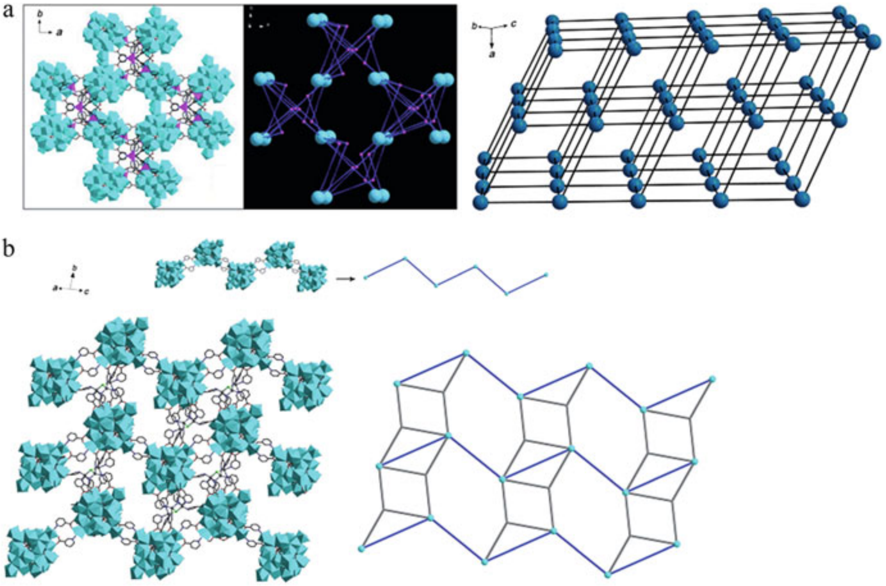

Fig. 18 (**a**) The 3D coordination structure constructed by {Dy_{26}} clusters and Cu centers and its perovskite-like topological structure; (**b**) the 2D coordination layer constructed by {Tb_{26}} clusters and $[Ag_3Cl]^{2+}$ bridges and its topological structure. Reproduced from [46] by permission of John Wiley & Sons Ltd

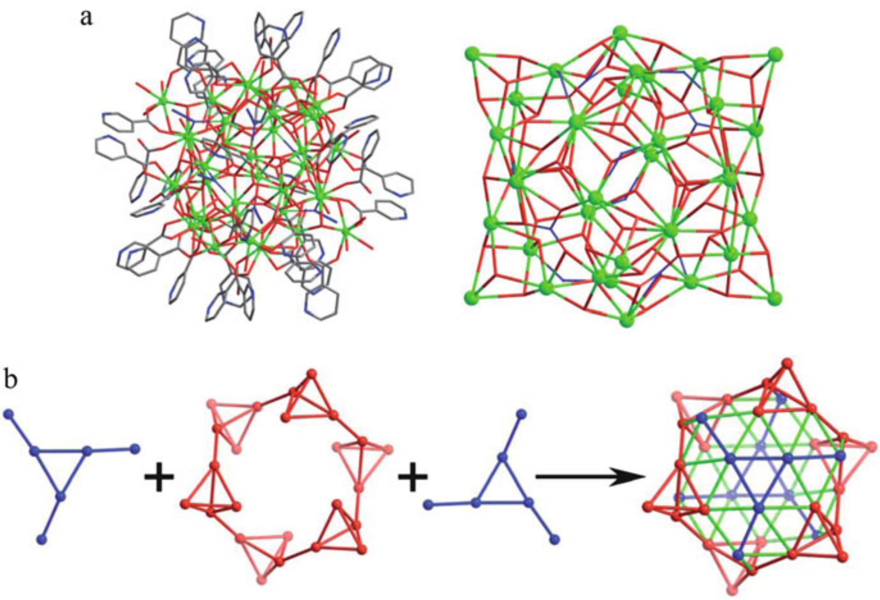

Fig. 19 (**a**) The 36-metal Gd(III) cluster; (**b**) illustration of the structure of Ln_{36} cluster. Reproduced from [47] by permission of The Royal Society of Chemistry

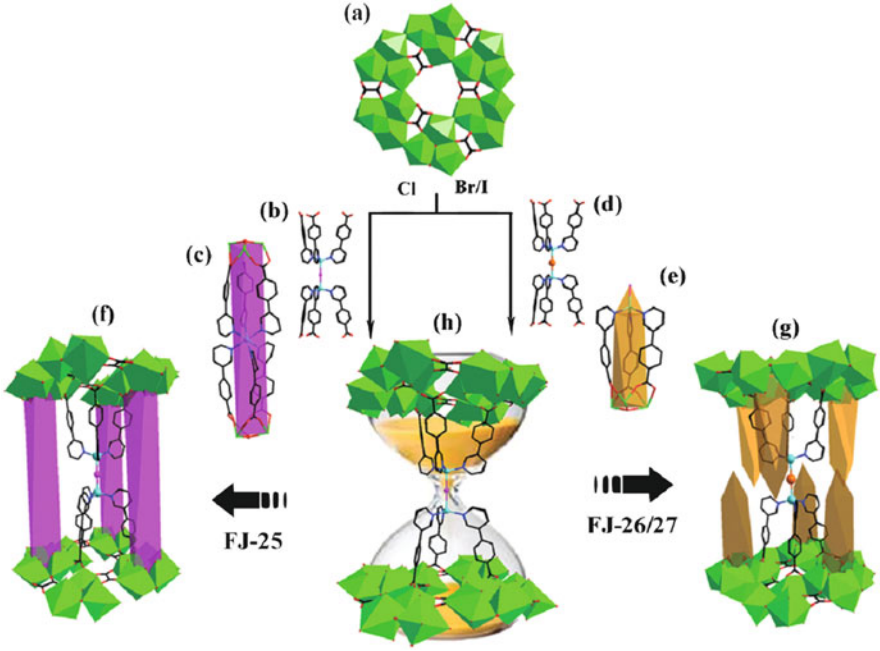

Fig. 20 View of the La_{18} TBU and auxiliary pillars in FJ-25 and FJ-26/27. Reproduced from [48] by permission of The Royal Society of Chemistry

2.4 *Cluster Organic Frameworks Constructed by 4-(3-Pyridyl)benzoic Acid*

Two series of wheel cluster organic frameworks (WCOFs), $La_6Cu_3ClL'_{12}(ox)_3(OH)_2 \cdot 8H_2O$ (FJ-25; ox = oxalate) and $La_6Cu_4X_3L'_{12}(ox)_3(OH)_2 \cdot H_3O$ (FJ-26/27; X = Br/I), are successfully made using 4-(3-pyridyl)benzoic acid (HL′) as ligands [48]. In these compounds, μ_3-OH bridge three La^{3+} ions to form edge-sharing trinuclear $[La_3(\mu_3\text{-}OH)]^{8+}$ (La_3) secondary building units (SBUs). The La_3 SBUs are linked by ox^{2-} ligands into a 6^3 graphene-like La_{18} wheel TBUs, TBUs are further linked by different kinds of pillars to give the whole frameworks (Fig. 20).

3 Summary

This chapter has provided a brief overview of the preparation and structures of lanthanide and Ln-TM cluster organic frameworks using rigid ligands under hydrothermal condition. These compounds show intriguing architectures with several structural types: (1) lanthanide clusters and coordination polymers linked via both Ln–O and Ln–N bonds and (2) Ln-TM heterometallic compounds constructed by lanthanide and different transition metal clusters/ions, in which these rigid ligands act as a linear bridge to form the heterometallic Cluster organic frameworks. The chapter broadens the research from discrete clusters to extended frameworks, which are different to the reported high-nuclearity Ln-TM clusters constructed by flexible ligands of Schiff-base and amino acids, in which the formation of mixed Ln-TM nanosized discrete clusters is usually observed with an investigation on the nature of the magnetic exchange interactions between 3d and 4f ions [3, 49]. The second ligand also plays an important role in the synthetic procedures, the inorganic anions can be used as templates or employed as surface modifiers inserted into the lanthanide cluster core backbone and improve the dimension of cluster cores. To date, the application of these compounds is mainly focused on magnetism and less involved in other aspects [50]. Further investigations in this area are necessary to use these large lanthanide and transition metal clusters to obtain porous cluster organic frameworks, and extend their uses in catalysis and adsorption processes.

Acknowledgements This work was supported by the NSFC (no. 91122028, 21571016, and 21471130), the NSFC for Distinguished Young Scholars (no. 20725101), and the NSF of Zhejiang Province (no. LY13B010002).

References

1. Chen L, Jiang FL, Zhou K, Wu MY, Hong MC (2015) Metal–organic frameworks based on lanthanide clusters. Struct Bond 163:145–184
2. Zhang Z, Zheng Z (2015) Nanostructured and/or nanoscale lanthanide metal-organic frameworks. Struct Bond 163:297–368
3. Kong XJ, Long LS, Zheng ZP, Huang RB, Zheng LS (2010) Keeping the ball rolling: fullerene-like molecular clusters. Acc Chem Res 43:201–209
4. Zhang SW, Cheng P (2015) Recent advances in the construction of lanthanide–copper heterometallic metal–organic frameworks. CrystEngComm 17:4250–4271
5. Roesky PW, Canseco-Melchor G, Zulys A (2004) A pentanuclear yttrium hydroxo cluster as an oxidation catalyst. Catalytic oxidation of aldehydes in the presence of air. Chem Commun 738–739
6. Bünzli J-CG, Piguet C (2002) Lanthanide-containing molecular and supramolecular polymetallic functional assemblies. Chem Rev 102:1897–1928
7. Shi W, Liu K, Cheng P (2015) Transition–lanthanide heterometal–organic frameworks: synthesis, structures, and properties. Struct Bond 163:231–264

8. Wang RY, Zheng ZP, Jin TZ, Staples RJ (1999) Coordination chemistry of lanthanides at "high" pH: synthesis and structure of the pentadecanuclear complex of europium(III) with tyrosine. Angew Chem Int Ed 38:1813–1815
9. Ma BQ, Zhang DS, Gao S, Jin TZ, Yan CH, Xu GX (2000) From cubane to supercubane: the design, synthesis, and structure of a three-dimensional open framework based on a Ln_4O_4 cluster. Angew Chem Int Ed 39:3644–3646
10. Wang WH, Tian HR, Zhou ZC, Feng YL, Cheng JW (2012) Two unusual chiral lanthanide-sulfate frameworks with helical tubes and channels constructed from interweaving two double-helical chains. Cryst Growth Des 12:2567–2571
11. Guo FS, Chen YC, Mao LL, Lin WQ, Leng JD, Tarasenko R, Orendáč M, Prokleška J, Sechovský V, Tong ML (2013) Anion-templated assembly and magnetocaloric properties of a nanoscale $\{Gd_{38}\}$ cage versus a $\{Gd_{48}\}$ barrel. Chem Eur J 19:14876–14885
12. Hu FL, Jiang FL, Zheng J, Wu MY, Pang JD, Hong MC (2015) Magnetic properties of 3D heptanuclear lanthanide frameworks supported by mixed ligands. Inorg Chem 54:6081–6083
13. Guo PH, Liu J, Wu ZH, Yan H, Chen YC, Jia JH, Tong ML (2015) Single-molecule-magnet behavior in a [2 × 2] grid Dy^{III}_4 cluster and a dysprosium-doped Y^{III}_4 cluster. Inorg Chem 54:8087–8092
14. Thielemann DT, Wagner AT, Rösch E, Kölmel DK, Heck JG, Rudat B, Neumaier M, Feldmann C, Schepers U, Bräse S, Roesky PW (2013) Luminescent cell-penetrating pentadecanuclear lanthanide clusters. J Am Chem Soc 135:7454–7457
15. Zhang L, Zhao L, Zhang P, Wang C, Yuan SW, Tang JK (2015) Nanoscale $\{Ln^{III}_{24}Zn^{II}_6\}$ triangular metalloring with magnetic refrigerant, slow magnetic relaxation, and fluorescent properties. Inorg Chem 54:11535–11541
16. Chang LX, Xiong G, Wang L, Cheng P, Zhao B (2013) A 24-Gd nanocapsule with a large magnetocaloric effect. Chem Commun 49:1055–1057
17. Canaj AB, Tzimopoulos DI, Philippidis A, Kostaki GE, Millios CJ (2012) A strongly blue-emitting heptametallic $[Dy^{III}_7]$ centered-octahedral single-molecule magnet. Inorg Chem 51:7451–7453
18. Joarder B, Mukherjee S, Xue SF, Tang JK, Ghosh SK (2014) Structures and magnetic properties of two analogous Dy_6 wheels with electron-donation and -withdrawal effects. Inorg Chem 53:7554–7560
19. Alexandropoulos DI, Fournet A, Cunha-Silva L, Mowson AM, Bekiari V, Christou G, Stamatatos TC (2014) Fluorescent naphthalene diols as bridging ligands in Ln^{III} cluster chemistry: synthetic, structural, magnetic, and photophysical characterization of Ln^{III}_8 "Christmas Stars". Inorg Chem 53: 5420–5422
20. Ren YX, Zheng XJ, Li LC, Yuan DQ, An M, Jin LP (2014) Three-dimensional frameworks based on dodecanuclear Dy – hydroxo wheel cluster with slow relaxation of magnetization. Inorg Chem 53:12234–12236
21. Addamo M, Bombieri G, Foresti E, Grillone MG, Volpe M (2004) Assembling process of charged nonanuclear cationic lanthanide(III) clusters assisted by dichromium decacarbonyl hydride. Inorg Chem 43:1603–1605
22. Sang RL, Xu L (2013) Unprecedented infinite lanthanide hydroxide ribbons $[Ln_3(\mu_3\text{-}OH)_3]_n^{6n+}$ in a 3-D metal-organic framework. Chem Commun 49:8344–8346
23. Dong J, Cui P, Shi PF, Cheng P, Zhao B (2015) Ultrastrong alkali-resisting lanthanide-zeolites assembled by $[Ln_{60}]$ nanocages. J Am Chem Soc 137:15988–15991
24. Kong XJ, Wu Y, Long LS, Zheng LS, Zheng Z (2009) A chiral 60-metal sodalite cage featuring 24 vertex-sharing $[Er_4(\mu_3\text{-}OH)_4]$ cubanes. J Am Chem Soc 131:6918–6919
25. Peng JB, Kong XJ, Zhang QC, Orendáč M, Prokleška J, Ren YP, Long LS, Zheng ZP, Zheng LS (2014) Beauty, symmetry, and magnetocaloric effect-four-shell keplerates with 104 lanthanide atoms. J Am Chem Soc 136:17938–17941
26. Cui Y, Yue Y, Qian G, Chen B (2012) Luminescent functional metal-organic frameworks. Chem Rev 112:1126–1162

27. Sun YQ, Zhang J, Chen YM, Yang GY (2005) Porous lanthanide-organic open frameworks with helical tubes constructed from interweaving triple-helical and double-helical chains. Angew Chem Int Ed 44:5814–5817
28. Zheng XJ, Jin LP, Gao S (2004) Synthesis and characterization of two novel lanthanide coordination polymers with an open framework based on an unprecedented $[Ln_7(\mu_3\text{-}OH)_8]^{13+}$ cluster. Inorg Chem 43:1600–1602
29. Lu JY (2003) Crystal engineering of Cu-containing metal–organic coordination polymers under hydrothermal conditions. Coord Chem Rev 246:327–347
30. Zhang MB, Zhang J, Zheng ST, Yang GY (2005) A 3D coordination framework based on linkages of nanosized hydroxo lanthanide clusters and copper centers by isonicotinate ligands. Angew Chem Int Ed 44:1385–1388
31. Cheng JW, Zhang J, Zheng ST, Yang GY (2008) Linking two distinct layered networks of nanosized $\{Ln_{18}\}$ and $\{Cu_{24}\}$ wheels through isonicotinate ligands. Chem Eur J 14:88–97
32. Gu XJ, Xue DF (2007) Surface modification of high-nuclearity lanthanide clusters: two tetramers constructed by cage-shaped $\{Dy_{26}\}$ clusters and isonicotinate linkers. Inorg Chem 46:3212–3216
33. Huang L, Han LJ, Feng WJ, Zheng L, Zhang ZB, Xu Y, Chen Q, Zhu DR, Niu SY (2010) Two 3D coordination frameworks based on nanosized huge Ln_{26} (Ln = Dy and Gd) spherical clusters. Cryst Growth Des 10:2548–2552
34. Chen L, Guo JY, Xu X, Ju WW, Zhang D, Zhu DR, Xu Y (2013) A novel 2-D coordination polymer constructed from high-nuclearity waist drum-like pure Ho_{48} clusters. Chem Commun 49:9728–9730
35. Wu M, Jiang F, Yuan D, Pang J, Qian J, AL-Thabaiti SA, Hong M (2014) Polymeric double anion template Er48 nanotubes. Chem Commun 50:1113–1115
36. Gu XJ, Xue DF (2007) 3D coordination framework $[Ln_4(\mu_3\text{-}OH)_2Cu_6I_5(IN)_8(OAc)_3]$ (IN = Isonicotinate): employing 2D layers of lanthanide wheel clusters and 1D chains of copper halide clusters. Inorg Chem 46:5349–5353
37. Cheng JW, Zhang J, Zheng ST, Zhang MB, Yang GY (2006) Lanthanide-transition-metal sandwich framework comprising $\{Cu_3\}$ cluster pillars and layered networks of $\{Er_{36}\}$ wheels. Angew Chem Int Ed 45:73–77
38. Cheng JW, Zheng ST, Yang GY (2008) Incorporating distinct metal clusters to construct diversity of 3D pillared-layer lanthanide-transition-metal frameworks. Inorg Chem 47:4930–4935
39. Fang WH, Cheng L, Huang L, Yang GY (2013) A series of lanthanide-based cluster organic frameworks made of heptanuclear trigonal-prismatic cluster units. Inorg Chem 52:6–8
40. Canaj AB, Tsikalas GK, Philippidis A, Spyros A, Milios CJ (2014) Heptanuclear lanthanide $[Ln_7]$ clusters: from blue-emitting solution-stable complexes to hybrid clusters. Dalton Trans 43:12486–12494
41. Fang WH, Yang GY (2014) Pillared-layer cluster organic frameworks constructed from nanoscale Ln_{10} and Cu_{16} clusters. Inorg Chem 53(11):5631–5636
42. Fang WH, Cheng JW, Yang GY (2014) Two series of sandwich frameworks based on two different kinds of nanosized lanthanide(III) and copper(I) wheel cluster units. Chem Eur J 20:2704–2711
43. Fang WH, Zhang L, Zhang J, Yang GY (2015) Construction of cluster organic frameworks with bnn hexagonal BN topologies. Chem Eur J 21:15511–15515
44. Fang WH, Zhang L, Zhang J, Yang GY (2016) Water stable homochiral cluster organic frameworks built by two kinds of large tetrahedral cluster units. Chem Eur J 22:2611–2615
45. Sen R, Hazra DK, Mukherjee M, Koner S (2011) Gd_{26} cluster consisting of distorted cubane cores: synthesis, structure and heterogeneous catalytic epoxidation of olefins. Eur J Inorg Chem 2826–2831
46. Zhang Y, Huang L, Miao H, Wan HX, Mei H, Liu Y, Xu Y (2015) Hydrothermal synthesis, structure, and optical properties of two nanosized $Ln_{26}@CO_3$ (Ln = Dy and Tb) cluster-based lanthanide–transition-metal–organic frameworks (Ln MOFs). Chem Eur J 21:3234–3241

47. Wu M, Jiang F, Kong X, Yuan D, Long L, Al-Thabaiti SA, Hong M (2013) Two polymeric 36-metal pure lanthanide nanosized clusters. Chem Sci 4:3104–3109
48. Fang WH, Zhang L, Zhang J, Yang GY (2016) Halogen dependent symmetry change in two series of wheel cluster organic frameworks built from La_{18} tertiary building units. Chem Commun 52:1455–1457
49. Zhou Y, Hong M, Wu X (2006) Lanthanide–transition metal coordination polymers based on multiple N and O-donor ligands. Chem Commun 135–143
50. Huang Y, Jiang F, Hong M (2009) Magnetic lanthanide–transition-metal organic–inorganic hybrid materials: from discrete clusters to extended frameworks. Coord Chem Rev 253:2814–2834